Green Chemistry

PAPER

View Article Online
View Journal

Cite this: DOI: 10.1039/d6gc01068g

Development of an efficient poly(3-hydroxybutyrate) production platform from lignocellulosic hydrolysates using a robust *Cupriavidus necator* RXI22 strain

Habin Sun,†[a] So Jeong Lee,†[a] Hyun-Joong Kim,[a] Hyeongmin Seo,[b] Jeongchan Lee,[a] Jung Ho Ahn,[a,c] Gyeongtaek Gong,[a,c] Youngsoon Um,[a,c] Kyoung Heon Kim [d] and Ja Kyong Ko *[a,c]

Lignocellulosic biomass represents a renewable and carbon-neutral feedstock for sustainable biomanufacturing of chemicals, fuels, and materials. In particular, microbial poly(3-hydroxybutyrate) (PHB) production from lignocellulosic hydrolysates offers a promising route toward reducing dependence on petroleum-based plastics and advancing circular bioeconomy strategies. The development of robust microbial hosts coupled with controllable bioprocessing is critical for efficient PHB production from lignocellulosic hydrolysates. In this study, efficient conversion of lignocellulosic hydrolysate sugar mixtures into PHB was established by using a genetically engineered *Cupriavidus necator* RXI22 strain as a microbial platform. *C. necator* RXI22, a glucose–xylose co-utilizer, exhibited relatively high cell density and PHB biosynthesis capabilities across diverse glucose–xylose ratios, underscoring its robustness toward the compositional variability inherent to lignocellulosic feedstocks. Systematic characterization of individual and combined hydrolysate-derived inhibitors further revealed that the key compounds limiting the fermentation performance are phenolic compounds, especially ferulic acid. When cultivated on hydrolysates from sugarcane bagasse and rice straw, *C. necator* RXI22 produced 6.1 and 7.0 g L^{-1} PHB, respectively, with yields of 0.29–0.30 g g^{-1}, representing the highest performance reported to date under comparable conditions. The results highlight that *C. necator* RXI22 is compatible with various industrially relevant lignocellulosic feedstocks. To mitigate inhibitory stress, a simple nutritional drop-in strategy was implemented, accelerating biomass accumulation and enhancing PHB productivity under inhibitor-rich conditions. Overall, this study establishes *C. necator* RXI22 as a promising platform for sustainable lignocellulose-to-PHB bioprocessing and provides insights for advancing eco-efficient biomanufacturing.

Received 19th February 2026,
Accepted 22nd May 2026

DOI: 10.1039/d6gc01068g

rsc.li/greenchem

Green foundation

1. This work evaluates the potential of *Cupriavidus necator* RXI22 to enable sustainable PHB production directly from lignocellulosic biomass, providing a bio-based route to displace petrochemical plastics. The strain's capability toward mixed sugars and inhibitors supports efficient valorization of renewable feedstocks.

2. *C. necator* RXI22 achieved PHB yields of 0.29–0.30 g g^{-1} on lignocellulosic hydrolysates, demonstrating compatibility with real biomass streams. Systematic inhibitor profiling identified phenolics as the dominant bottleneck, and a nutrient supplementation strategy provided measurable improvements under model inhibitor stresses.

3. Future work is recommended to integrate metabolic engineering to enable *in situ* detoxification and conversion of inhibitors, reducing reliance on intensive pretreatment. Process optimization and greener PHB recovery methods will further enhance environmental performance and overall sustainability.

[a]*Clean Energy Research Center, Korea Institute of Science and Technology (KIST), Seoul 02792, Republic of Korea. E-mail: jkko@kist.re.kr*
[b]*Department of Chemical and Biochemical Engineering, University of Iowa, Iowa City, Iowa 52242, USA*
[c]*Division of Energy and Environment Technology, KIST School, University of Science and Technology, Seoul 02792, Republic of Korea*
[d]*Department of Biotechnology, Korea University, Seoul 02841, Republic of Korea*
†These authors equally contributed to this work.

1. Introduction

Severe environmental pollution associated with plastic waste has become a global concern, driving intensified efforts to develop sustainable material alternatives and accelerating interest in biodegradable plastics to replace conventional petroleum-based polymers.[1] Biodegradable plastics support circu-

lar economy concepts, while bio-based plastics derived from renewable resources can reduce environmental burdens and enable more sustainable material cycles.[2] In this context, polyhydroxyalkanoates (PHAs), a class of microbially synthesized polyesters, have attracted increasing attention as sustainable biopolymers due to their high biocompatibility and mechanical properties suitable for both industrial and biomedical applications.[3,4]

The economic and environmental viability of PHA production strongly depends on the use of renewable and low-cost feedstocks. Among various candidates, lignocellulosic biomass has been recognized as a key resource for next-generation biomanufacturing because of its abundance and lack of competition with food supplies.[5,6] Generated in large quantities from agricultural and forestry residues, lignocellulosic biomass offers significant potential for lowering carbon source costs in biomanufacturing processes. Structurally, it consists of cellulose, hemicellulose, and lignin, which can be converted into fermentable sugars, such as glucose and xylose, *via* appropriate pretreatment and hydrolysis processes.[6] These sugars can subsequently serve as substrates for microbial synthesis of value-added products, including biodegradable PHAs.[7,8] Importantly, the valorization of lignocellulosic biomass contributes to decreased reliance on fossil resources and reduced carbon emissions.[9]

Among microbial platforms for PHA production from lignocellulosic sugars, *Cupriavidus necator* (also referred to as *Ralstonia eutropha*) has been extensively studied due to its broad substrate utilization capability and exceptional poly(3-hydroxybutyrate) (PHB) accumulation capacity.[10] Nevertheless, the practical application of *C. necator* in lignocellulose-based processes has been largely constrained by its inefficient utilization of glucose and xylose, the major monomeric sugars in lignocellulosic hydrolysates.[11,12] For example, wild-type *C. necator* is unable to consume glucose and/or xylose due to the lack of a glucose transporter and a xylose assimilation pathway.[13,14] To address this limitation, a glucose–xylose co-utilizer *C. necator* RXI22 was previously developed *via* chromosomal integration of the xylose isomerase (XI) pathway followed by adaptive laboratory evolution (ALE).[14] While the engineered phenotype enabled simultaneous conversion of glucose and xylose into PHB, their fermentation performance in lignocellulosic hydrolysates remained unexplored.

Most of the lignocellulosic hydrolysates contain inhibitory compounds generated during the upstream biomass pretreatments.[15,16] Their composition also varies with biomass feedstock and pretreatment severity,[17] further complicating robust microbial PHB production. Despite these technical challenges, most studies have primarily focused on strain development or sugar utilization in synthetic media, providing limited understanding of strain performance under industrially relevant hydrolysate conditions. Notably, a substantial performance disparity exists between synthetic media and actual lignocellulosic hydrolysates. While several strains have shown promise in synthetic media, PHA production from raw biomass-derived hydrolysates suffers from significantly lower titers and productivity.[18] This discrepancy is attributed not only to varying sugar concentrations but also to the inherent chemical complexity of the hydrolysates, specifically the synergistic toxicity of pretreatment byproducts, which remains a major hurdle for the commercialization of lignocellulosic PHAs.

Accordingly, the present study aims to establish a robust fermentation strategy for enhanced PHB production by systematically investigating the metabolic behavior of *C. necator* RXI22 in actual lignocellulosic hydrolysates. To achieve this, we first characterized the strain's performance under varying mixed-sugar and carbon-to-nitrogen (C/N) conditions, followed by validation using real lignocellulosic biomass hydrolysates. Furthermore, the impacts of major inhibitory compounds were quantitatively assessed to identify key factors limiting fermentation efficiency. Finally, the potential of nutritional supplementation was investigated as a strategy to improve strain robustness under inhibitory conditions, providing practical insights into the challenges and opportunities of designing sustainable biomass-based PHB production processes.

2. Materials and methods

2.1. Strain and media

The engineered strain *C. necator* RXI22 was employed as the microbial platform for PHB production. RXI22 originates from *C. necator* NCIMB 11599 and was rewired for mixed-sugar metabolism by replacing the native *norB2* locus with the xylose isomerase (*xylA*) and xylulokinase (*xylB*) genes from *Escherichia coli* MG1655, followed by adaptive laboratory evolution (ALE) to improve xylose assimilation.[14] Seed cultures were initiated from Luria–Bertani (LB) agar plates and grown in LB broth at 30 °C. For PHB production, cells were cultivated in a minimal medium containing 1.5 g L^{-1} KH_2PO_4, 4.5 g L^{-1} $Na_2HPO_4{\cdot}2H_2O$, 80 mg L^{-1} $MgSO_4{\cdot}7H_2O$, 1 mg L^{-1} $CaSO_4{\cdot}2H_2O$, 0.75–4 g L^{-1} $(NH_4)_2SO_4$, 0.5 g L^{-1} $NaHCO_3$, 4 mg L^{-1} $FeSO_4{\cdot}7H_2O$, 0.1 mg L^{-1} $ZnSO_4{\cdot}7H_2O$, and 0.6 mg L^{-1} $NiSO_4{\cdot}6H_2O$. Glucose and xylose were supplemented at concentrations specified for each experiment.

2.2. Shake-flask cultivation

Single colonies from LB agar were transferred to LB broth and grown for 24 h at 30 °C and 200 rpm. Cells were harvested at 4200 rpm for 10 min, washed twice with minimal medium, and inoculated into 100 mL flasks containing 20 mL minimal medium (initial OD_{600} = 0.2). Media containing lignocellulosic hydrolysates were adjusted to pH 7.3 with 1 M NaOH. Cell growth was monitored every 24 h using a UV-visible spectrophotometer (Cary 60, Agilent Technologies, CA, USA). Tryptophan and nicotinic acid (Sigma-Aldrich, St Louis, MO, USA) were supplemented (0.05–2 g L^{-1}) when indicated to improve hydrolysate fermentation.

2.3. Inhibitor tolerance assay

For inhibitor tolerance tests, micro-scale cultivations were carried out in 96-well plates containing 190 μL of medium sup-

plemented with 5 g L^{-1} glucose or xylose and 1 g L^{-1} $(NH_4)_2SO_4$. Each well was inoculated with 10 μL of LB preculture and incubated at 30 °C and 200 rpm for 48 h. Cell density was measured at 600 nm using a Spark multimode microplate reader (Tecan, Switzerland). Stock solutions of acetic acid (as sodium acetate), furfural, and 5-hydroxymethylfurfural (HMF) were prepared in distilled water, while *p*-coumaric acid and ferulic acid were dissolved in ethanol due to limited aqueous solubility. All stock solutions were sterilized by filtration prior to supplementation.

2.4. Preparation of lignocellulosic hydrolysates

Lignocellulosic hydrolysates were generated from sugarcane bagasse (SB) and rice straw (RS) using dilute acid pretreatment followed by enzymatic hydrolysis, adapted from Ko *et al.* (2019).[19] Briefly, 37 g of dried biomass was suspended in 250 mL of 1% (w/v) H_2SO_4 and subjected to hydrothermal pretreatment by autoclaving at 121 °C for 30 min. The pretreated slurry was then adjusted to pH 5.0 and hydrolyzed with Cellic CTec2 (Novozyme, North America Inc., Franklinton, NC) at 50 °C for 96 h. The liquid fraction was separated from the residual solids containing insoluble lignin and sterilized by filtration for use in fermentation experiments. The resulting SB hydrolysate contained 24.4 g L^{-1} glucose, 24.7 g L^{-1} xylose, 3.3 g L^{-1} acetic acid, and 1.0 g L^{-1} total phenolics, whereas the RS hydrolysate contained 23.9 g L^{-1} glucose, 14.4 g L^{-1} xylose, 1.5 g L^{-1} acetic acid, and 1.0 g L^{-1} total phenolics. Total phenolics were quantified as representative compounds of the soluble inhibitors derived from lignin during the pretreatment and saccharification processes.

The total nitrogen content in the lignocellulosic hydrolysates was determined using a modified alkaline persulfate digestion method. Briefly, the samples were digested with alkaline potassium persulfate (0.5 M $K_2S_2O_8$ in 0.5 M NaOH) at 120 °C for 60 min, followed by neutralization, and the resulting ammonium was quantified using the indophenol blue assay. The endogenous nitrogen concentrations in the SB and RS hydrolysates were determined to be 0.47 and 0.43 g L^{-1}, respectively.

2.5. Quantification of sugars and hydrolysate inhibitors

Glucose, xylose, acetic acid, furfural and HMF concentrations in the culture supernatant were quantified by high-performance liquid chromatography (HPLC) using an Agilent 1260 Infinity system (Agilent Technologies, CA, USA) equipped with a HiPlex-H column (300 × 7.7 mm, Agilent Technologies, CA, USA). The mobile phase consisted of 5 mM H_2SO_4 at a flow rate of 0.6 mL min^{-1}. Sugars were detected using a refractive index detector, whereas acetic acid, furfural, and HMF were monitored using a UV detector at 210 nm.

For the total phenolics assay, 0.5 mL of the sample diluted in distilled water was mixed with 0.25 mL of Folin–Ciocalteu reagent and 1.25 mL of 20% (w/v) sodium carbonate, followed by incubation at room temperature for 40 min. The absorbance of the reaction mixture was measured at 725 nm using a UV-visible spectrophotometer (Cary 60, Agilent Technologies, CA, USA). The total phenolic content was calculated using a standard curve generated with gallic acid solutions.

2.6. PHB quantification

Intracellular PHB was quantified following methanolysis of lyophilized cells and analysis by gas chromatography (GC). Cell pellets obtained by centrifugation were washed with distilled water, frozen at −80 °C, and subsequently freeze-dried (Operon, Gimpo, Republic of Korea). A known amount of dried biomass was subjected to acidic methanolysis using methanol–sulfuric acid, with chloroform as the extraction solvent and methyl benzoate serving as the internal standard. The resulting methyl esters were analyzed on a GC system equipped with a flame ionization detector (FID) (Agilent Technologies, CA, USA) and an HP-5MS capillary column (30 m × 0.32 mm × 0.25 μm). The injector temperature was maintained at 250 °C. The oven temperature program consisted of an initial hold at 40 °C for 5 min, followed by a ramp to 280 °C at 10 °C min^{-1}, and a final hold for 2 min. The detector temperature was set to 300 °C.

2.7. Fabrication of PHB films

Dried cell biomass (100 mg) was suspended in 5 mL of chloroform and 5 mL of sodium hypochlorite solution. The mixture was incubated at 30 °C with shaking at 200 rpm overnight to enable cell lysis and PHB extraction. Phase separation was subsequently achieved by centrifugation, after which the organic (chloroform) phase was carefully collected and transferred onto a glass plate, where the solvent was allowed to evaporate under a fume hood to obtain PHB films. The thermal properties of the recovered PHB films were analyzed using differential scanning calorimetry (DSC 4000, PerkinElmer, USA). Samples (4–6 mg) were encapsulated in aluminum pans and subjected to heating–cooling cycles ranging from −60 °C to 200 °C under a nitrogen atmosphere, with a 5 min holding step at 200 °C. The melting temperature (T_m) and glass transition temperature (T_g) were determined from the second heating cycle.

3. Results and discussion

3.1 Optimization of the C/N ratio for PHB production by *C. necator* RXI22 under mixed-sugar conditions

C. necator is a well-known PHB-producing bacterium, and nutrient limitation, particularly nitrogen limitation, is commonly employed to suppress cell growth while enhancing PHB accumulation.[20,21] Under nitrogen-limited conditions, imbalances between carbon and nitrogen availability alter intracellular redox states and carbon fluxes,[22] favoring nicotinamide adenine dinucleotide phosphate (NADPH) availability and reducing free CoA formation, thereby redirecting carbon toward PHB biosynthesis.[23] Before examining fermentation performance in lignocellulosic hydrolysates, cultivation conditions were first investigated using a mixed-sugar model system to characterize the physiological response of *C. necator*

RXI22. To this end, the effect of the carbon-to-nitrogen (C/N) ratio on PHB production was investigated by varying the concentration of $(NH_4)_2SO_4$ (1–4 g L^{-1}) in a medium containing a 1 : 1 mixture of glucose and xylose at a total sugar concentration of 30 g L^{-1}. These conditions corresponded to C/N ratios of 66, 44, 33, 22, and 16.5. Among the conditions tested, a C/N ratio of 44 yielded the highest biomass concentration (12.0 g L^{-1}) and PHB production (9.7 g L^{-1}), representing the maximum PHB titer observed (Fig. 1). In contrast, a higher C/N ratio of 66 led to the highest PHB content (85.4 wt%) but lower biomass formation. This inverse relationship highlights the dependence of cell growth and intracellular PHB accumulation on nitrogen availability.

Comparable trends have been reported in previous studies, although the C/N ratio yielding optimal PHB production differs depending on both the microbial host and the carbon source. For example, Yang *et al.* (2010)[24] reported that a C/N ratio of 80 maximized PHB content in *C. necator* H16 cultivated on volatile fatty acids, whereas a lower ratio of 40 favored biomass formation. Similarly, Al-Battashi *et al.* (2019)[25] observed that higher C/N ratios enhanced PHB accumulation but reduced cell growth in *Burkholderia sacchari* DSM 17165 grown on a waste office paper hydrolysate as the carbon source, leading to the selection of a C/N ratio of 20 as optimal. These findings indicate that although C/N ratios between approximately 20 and 60 are frequently reported, the optimal range is highly influenced by strain-specific metabolism, carbon substrate, and cultivation conditions.[11,24,25] Consistent with these observations, *C. necator* RXI22 exhibited a C/N ratio-dependent balance between biomass formation and PHB accumulation under glucose–xylose mixed sugar conditions. Taking both PHB titer and cell growth into account, a C/N ratio of 44 was used in subsequent fermentation experiments.

3.2 Effect of the G/X ratio on PHB production using *C. necator* RXI22

The glucose–xylose composition in lignocellulosic hydrolysates varies widely depending on biomass type and pretreatment conditions.[17] Consequently, the ability to maintain robust cell growth and stable PHB productivity under fluctuating lignocellulosic sugar ratios is essential for economically viable biomanufacturing. To assess this capability, PHB production by *C. necator* RXI22 was evaluated using 30 g L^{-1} mixed sugars with glucose–xylose (G–X) ratios ranging from 5 : 1 to 1 : 5 (Fig. 2).

C. necator RXI22 simultaneously consumed both sugars across all tested conditions, achieving strong growth (OD_{600} ≥ 40, up to 54) and complete glucose depletion with more than half of the xylose utilized within 96 h (Fig. 2A–E). PHB accumulation remained consistently high, yielding ≥75 wt% PHB content and 7.5–11.3 g L^{-1} titers, corresponding to overall yields of 0.33–0.46 g g^{-1} (Fig. 2F). Compared with previously reported strains capable of utilizing both glucose and xylose, *C. necator* RXI22 exhibited markedly superior robustness and efficiency (Table 1). Previous studies often showed high PHB content only at specific sugar ratios or achieved limited biomass, resulting in PHB titers of 1.3–9.6 g L^{-1}. For example, *C. necator* NCIMB 11599 carrying plasmid-based *xylA* and *xylB* produced only 1.3 g L^{-1} PHB under the G10X10 condition,[26] whereas *C. necator* RXI22 achieved 10.7 g L^{-1} at G15X15. Similarly, *C. necator* RXI22 produced a 1.8-fold higher PHB titer than *Halomonas nigrificans* X339 under a comparable mixed-sugar condition (G20X10).[27] In addition, *C. necator* RXI22 outperformed *Schlegelella thermodepolymerans*, which exhibited lower PHB yields (0.29–0.30 g g^{-1}),[28] by consistently maintaining higher yields of 0.33–0.46 g g^{-1}. These comparisons highlight the exceptional carbon conversion efficiency of *C. necator* RXI22 across diverse glucose–xylose compositions.

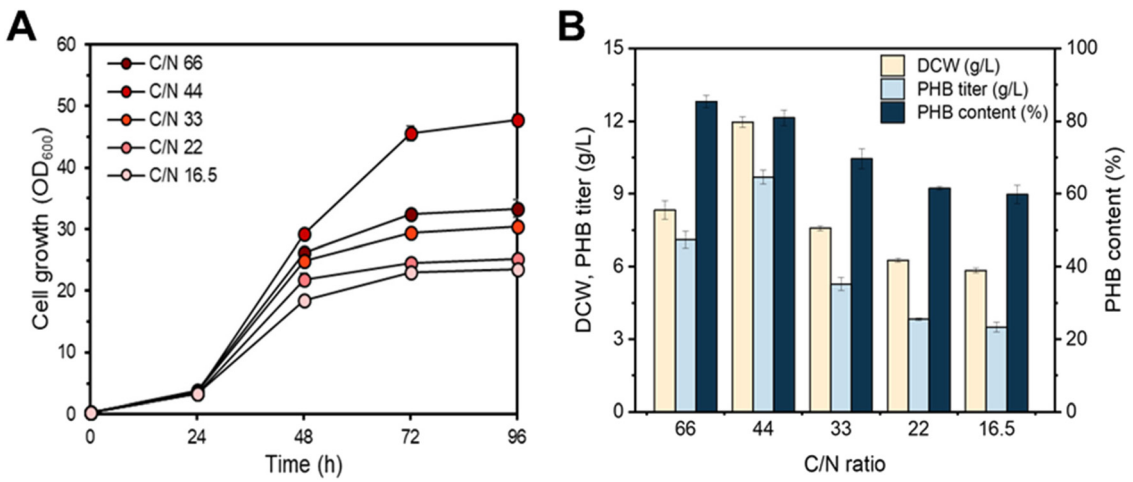

Fig. 1 Optimization of the carbon-to-nitrogen (C/N) ratio for PHB production by *C. necator* RXI22 under mixed-sugar fermentation conditions. The strain was cultivated on a mixed-sugar substrate consisting of glucose (15 g L^{-1}) and xylose (15 g L^{-1}) with varying $(NH_4)_2SO_4$ concentrations (1–4 g L^{-1}). (A) Cell growth profiles and (B) dry cell weight (DCW), PHB titer, and yield measured after 96 h of cultivation. Data are presented as mean ± standard deviation of three biological replicates.

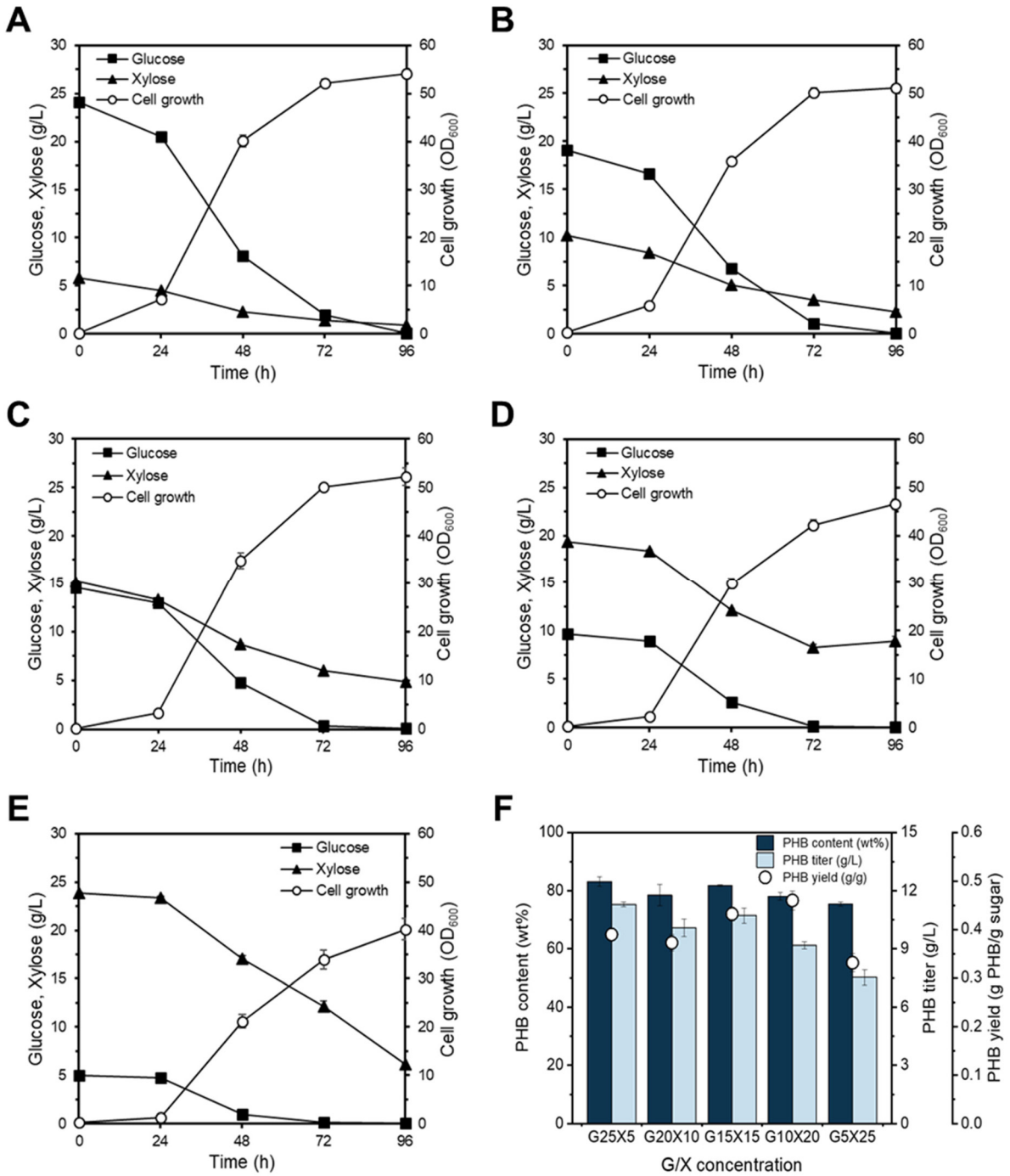

Fig. 2 Fermentation profiles of *C. necator* RXI22 under varying glucose–xylose ratios. Cell growth and sugar consumption profiles of RXI22 cultivated with mixed sugars at (A) 25 g L^{-1} glucose and 5 g L^{-1} xylose (G25X5), (B) 20 g L^{-1} glucose and 10 g L^{-1} xylose (G20X10), (C) 15 g L^{-1} glucose and 15 g L^{-1} xylose (G15X15), (D) 10 g L^{-1} glucose and 20 g L^{-1} xylose (G10X20), and (E) 5 g L^{-1} glucose and 25 g L^{-1} xylose (G5X25). (F) PHB content, titer, and yield obtained after 96 h of cultivation under each corresponding condition. Total sugar concentration was fixed at 30 g L^{-1} in all conditions. Data are presented as mean ± standard deviation of three biological replicates.

Although *C. necator* RXI22 maintained high PHB production under all mixed-sugar ratios, substrate composition influenced sugar utilization and biomass formation. Higher glucose fractions led to increased cell densities, likely reflecting the higher metabolic accessibility and energy efficiency of glucose relative to xylose.[14] Specifically, glucose is directly channeled into glycolysis, whereas xylose requires additional metabolic steps before entering central carbon metabolism *via* the pentose phosphate pathway (PPP). This extended catabolic route, combined with the inherently lower metabolic flux, gen-

Table 1 PHB production from mixed sugars by various PHB-producing microorganisms

Strain	Strain description	Substrate	DCW (g L^{-1})	PHB content (wt%)	PHB yield (g g^{-1})	PHB titer (g L^{-1})	Ref.
C. necator RXI22	NCIMB 11599 derivative; chromosomal integration of P_{j5}-*xylAB*$_{Ec}$-rrnBT1 at the *norB2* locus; ALE-evolved	G25, X5	13.6	83.2	0.39	11.3	This study
		G20, X10	12.8	78.5	0.37	10.1	
		G15, X15	13.1	81.8	0.43	10.7	
		G10, X20	11.6	78.1	0.46	9.2	
		G5, X25	10.1	75.4	0.33	7.5	
B. megaterium R11	Wild type	G33, X17	16.9	56.7	0.21	9.6	30
B. sacchari DSM 17165	Wild type	X20	5.2	43.0		2.2	31
		G10, X10	4.8	49.0		2.4	
H. nigrificans X339	Wild type	G30	16.0	48.9		7.8	27
		G20, X10	12.6	44.1		5.6	
		X30	10.7	24.2		2.4	
S. thermodepolymerans DSM 15344	Wild type	X20	6.5	77.4	0.30	5.1	28
		G4, X16	6.4	74.3	0.30	4.8	
		G10, X10	6.0	74.6	0.29	4.5	
C. necator NCIMB 11599 (pKM212-XylAB)	NCIMB 11599 derivative; harboring pKM212-*XylAB*	G15, X5	1.7	93.3		1.5	26
		G10, X10	1.5	86.6		1.3	

G, glucose; X, xylose; DCW, dry cell weight.

erally results in reduced ATP generation efficiency compared to glucose metabolism.[29] Consistent with these metabolic constraints, the specific consumption rate of glucose (0.072 g g^{-1} h^{-1}) was higher than that of xylose (0.044 g g^{-1} h^{-1}) under the G15X15 condition. Consequently, increasing the xylose proportion reduced overall sugar consumption despite continued co-utilization, indicating composition-dependent substrate uptake behavior. These observations suggest that further optimization of xylose transport and downstream pathway flux will be necessary to achieve more efficient co-utilization. Nevertheless, PHB yields remained above 0.35 g g^{-1} under most conditions, suggesting that *C. necator* RXI22 effectively channels the carbon flux toward PHB synthesis regardless of sugar composition. This metabolic robustness provides a notable advantage for lignocellulosic bioprocesses, where variability in hydrolysate sugar composition is unavoidable.

3.3. PHB production from lignocellulosic biomass hydrolysates

Given the strong performance of *C. necator* RXI22 across diverse G/X ratios using model sugars, it remains uncertain whether this robustness extends to actual lignocellulosic hydrolysates. Unlike model sugar mixtures, hydrolysates generated from dilute acid pretreatment followed by enzymatic saccharification contain not only fermentable sugars but also inhibitory compounds such as organic acids, furans, and phenolics derived from lignocellulosic biomass.[32] To bridge the findings from model systems to realistic conditions, the C/N ratio was maintained at 44, the optimized value identified in previous sections to support maximum PHB accumulation. Furthermore, the demonstrated robustness of RXI22 across various G/X ratios suggested its potential to effectively process the diverse sugar profiles of actual biomass feedstocks. Two hydrolysates, derived from sugarcane bagasse (SB) and rice straw (RS), were examined. SB contained 14.5 g L^{-1} glucose and 14.8 g L^{-1} xylose, while RS contained 18.7 g L^{-1} glucose and 10.4 g L^{-1} xylose, with both also comprising acetic acid, furfural, 5-hydroxymethylfurfural (HMF), and phenolic compounds at distinct levels (Table 2). Although the inclusion of endogenous nitrogen from the hydrolysates slightly reduced the actual C/N ratio to 33–36, the C/N ratio was formally defined by the added ammonium sulfate. This ensured a direct and consistent comparison with the hydrolysate mimics (sugars-only controls), particularly as the bioavailability and specific forms of complex nitrogenous compounds within the hydrolysates remain uncertain.

Fermentations using each hydrolysate were compared with hydrolysate mimics (containing comparable sugar mixtures only) (Fig. 3). *C. necator* RXI22 was able to consume mixed sugars in both hydrolysates, reaching OD_{600} values of 39 (SB hydrolysate) and 41 (RS hydrolysate), corresponding to biomass concentrations of 9.8 g L^{-1} and 10.3 g L^{-1}, respectively (Fig. 3A and B). Nevertheless, the presence of inhibitors clearly reduced fermentation performance. Relative to sugar-mimic controls, the final OD_{600} was reduced by 23–25%, and the PHB titer reduced to 6.1–7.0 g L^{-1} by 43 and 37%, respectively (Fig. 3C and D). PHB yields also declined from 0.42–0.43 g g^{-1} in model sugars to 0.29–0.30 g g^{-1} in both hydrolysate cultivations (Fig. 3E). Although a minor variance

Table 2 Composition of lignocellulosic hydrolysate-supplemented media used in this study

Components (g L^{-1})	Sugarcane bagasse	Rice straw
Glucose	14.5	18.7
Xylose	14.8	10.4
Acetic acid	2.1	1.3
Furfural	0.017	0.003
5-Hydroxymethylfurfural	0.84	0.03
Phenolic compounds	0.6	0.6

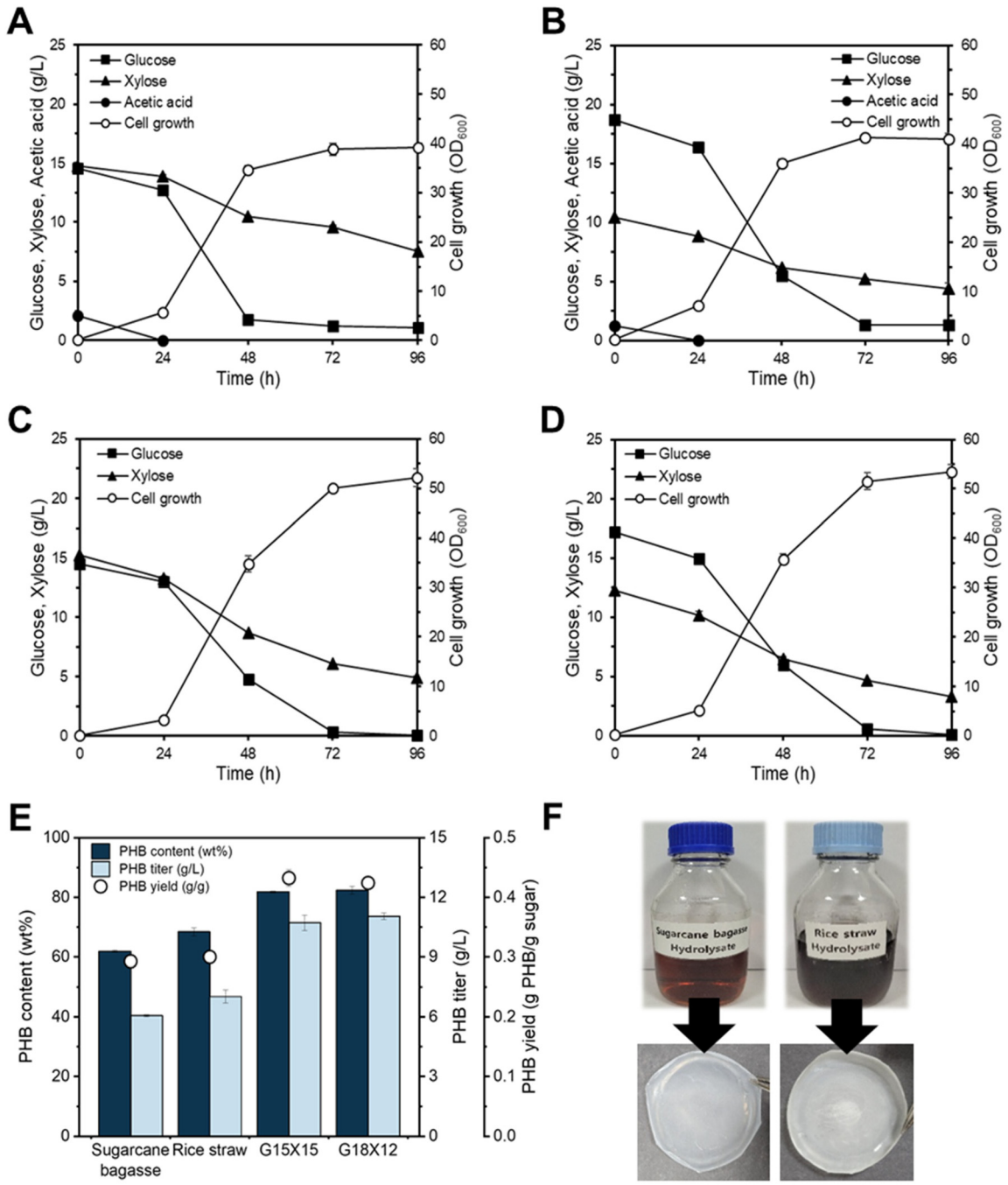

Fig. 3 Fermentation performance of *C. necator* RXI22 on lignocellulosic hydrolysates and the corresponding mixed-sugar mimics. Growth and sugar utilization profiles of *C. necator* RXI22 cultivated with (A) the sugarcane bagasse (SB) hydrolysate, (B) the rice straw (RS) hydrolysate, (C) an SB-mimic medium containing 15 g L^{-1} glucose and 15 g L^{-1} xylose, and (D) an RS-mimic medium containing 18 g L^{-1} glucose and 12 g L^{-1} xylose. (E) PHB content, titer, and yield obtained after 96 h under each respective condition. (F) PHB films prepared from polymers recovered after 96 h of cultivation using lignocellulosic hydrolysates. Mixed-sugar mimics were formulated to reproduce the glucose–xylose compositions of the corresponding hydrolysates. Data are presented as mean ± standard deviation of three biological replicates.

existed in initial xylose concentrations between the RS hydrolysate and its mimic, the overall inhibitory trends remained clear as substrate consumption reached a metabolic plateau despite the presence of residual sugars (Fig. 3D). While the final PHB titers obtained from the two hydrolysates were comparable (6.1–7.0 g L^{-1}), this similarity does not imply identical inhibitory mechanisms. Instead, it suggests that the distinct combination of inhibitors in each feedstock resulted in a similar cumulative impact on overall PHB production efficiency under the tested conditions.

The recovered PHB was further processed into films, demonstrating the material applicability of PHB produced from lignocellulosic hydrolysates (Fig. 3F). To evaluate the physicochemical properties of the produced biopolymer, its thermal behavior was characterized *via* DSC. The PHB films derived from SB and RS hydrolysates exhibited melting temperatures (T_m) of 162.1 °C and 164.1 °C, respectively, and glass transition temperatures (T_g) of −4.2 °C and −3.0 °C, respectively. These thermal characteristics are comparable to previously reported values for PHB produced from sugar industry waste (T_m = 161.7 °C, T_g = −2.8 °C),[33] indicating that the PHB films exhibited thermal behavior comparable to that of conventional PHB.

Even with the performance reduction relative to the model sugar conditions, *C. necator* RXI22 remained highly competitive when compared with previously reported strains fermenting lignocellulosic hydrolysates in flasks (Table 3). Among *C. necator* strains, RXI22 showed higher PHB yields (0.29 g g^{-1}) than wild-type NCIMB 11599 (0.21 g g^{-1} from waste office paper) and produced substantially higher PHB titers than Reh06 (3.8 g L^{-1} from corn stover).[34] Other microorganisms such as *Escherichia coli* phaP1,3, *Bacillus megaterium* PNCM 1890, and *Halomonas* sp. YLGW01 also displayed lower or comparable titers (3.1–6.1 g L^{-1}).[7,8,18] Overall, although *C. necator* RXI22 outperformed other reported strains in lignocellulosic hydrolysate fermentations, its reduced performance compared with model sugars underscores the need to clarify how individual inhibitory compounds contribute to PHB biosynthesis limitations.

3.4. Effects of inhibitory compounds in lignocellulosic hydrolysates on *C. necator* RXI22

To examine how hydrolysate-derived inhibitors affect *C. necator* RXI22, a tolerance assessment was conducted using 96-well plate cultivations with glucose or xylose as the sole carbon source. Concentration ranges for each inhibitor were determined based on their levels in the SB and RS hydrolysates, and growth responses were evaluated accordingly (Fig. S1 and S2). Acetic acid exhibited clear sugar-dependent effects: it inhibited growth under glucose conditions but enhanced growth when xylose was used. This contrasting behavior aligns with reports that acetic acid suppresses glucose phosphotransferase system (PTS)-mediated uptake and disrupts the acetyl-CoA flux during glucose catabolism,[37] whereas under xylose metabolism, primarily *via* the pentose phosphate pathway, it can act as an auxiliary substrate boosting central metabolism and biosynthetic gene expression.[38,39] Furfural and HMF, in contrast, showed minimal inhibitory effects across the tested concentrations. Phenolic compounds exerted the strongest inhibition, suppressing growth in a concentration-dependent manner under both glucose and xylose. *p*-Coumaric acid and ferulic acid, the dominant phenolic compounds generated during SB and RS biomass pretreatment,[40–42] both reduced cell growth, with ferulic acid exhibiting the most pronounced toxicity. These observations suggested that phenolic compounds, particularly ferulic acid, were likely the major contributors to the growth inhibition.

Although inhibitor tolerance was initially evaluated under single-sugar conditions, actual lignocellulosic hydrolysates contain both glucose and xylose, and the presence of mixed sugars can alter metabolic fluxes and lead to inhibitor responses that differ from those observed with a single carbon source.[43] To evaluate inhibitor effects under conditions more reflective of actual hydrolysates, mixed-sugar cultures mimicking the SB hydrolysate composition (acetic acid 1.5 g L^{-1}, furfural 0.02 g L^{-1}, HMF 0.5 g L^{-1}, phenolics 0.5 g L^{-1}) were tested. Under these conditions, RXI22 exhibited inhibitor-specific reductions in growth, sugar utilization, and PHB production (Fig. 4).

Acetic acid had minimal impact on glucose and xylose consumption, yet PHB titers and yields were reduced by 9% and 14%, respectively, compared with the control, indicating that even mild perturbations to the carbon flux can negatively affect PHB biosynthesis (Fig. 4A and J). Furfural and HMF

Table 3 PHB production from lignocellulosic biomass hydrolysates by various PHB-producing microorganisms

Strain	Lignocellulosic biomass	Inhibitory compounds (g L^{-1})	Glucose (g L^{-1})	Xylose (g L^{-1})	PHB content (wt%)	PHB yield (g g^{-1})	PHB titer (g L^{-1})	Ref.
C. necator RXI22	Rice straw	1.3 acetic acid, 0.003 furfural, 0.03 HMF, 0.6 phenolics	18.7	10.4	68.4	0.30	7.0	This study
	Sugarcane bagasse	2.1 acetic acid, 0.017 furfural, 0.84 HMF, 0.6 phenolics	14.5	14.8	61.9	0.29	6.1	This study
C. necator Reh06	Corn stover	0.21 ferulic acid, 1.25 *p*-coumaric acid	21.5	7.8	—	—	3.8	35
C. necator NCIMB 11599	Waste office paper	0.14 phenolics	22.7	1.8	57.5	0.21	4.5	34
R. eutropha ATCC17699	Hemp hurd biomass	—	42.0	11.5	56.3	0.25	13.4	36
B. megaterium PNCM 1890	Sugarcane bagasse	—	13.9	4.6	—	0.31	6.1	8
E. coli phaP1,3	*Miscanthus*	0.005 acetic acid	30.0	1.0	—	—	3.9	7
Halomonas sp. YLGW01	Pine tree	0.2 acetic acid, 0.03 formic acid, 0.02 levulinic acid, 0.02 HMF, 0.05 furfural	28.7	1.3	61.7	—	3.1	18

HMF, 5-hydroxymethylfurfural.

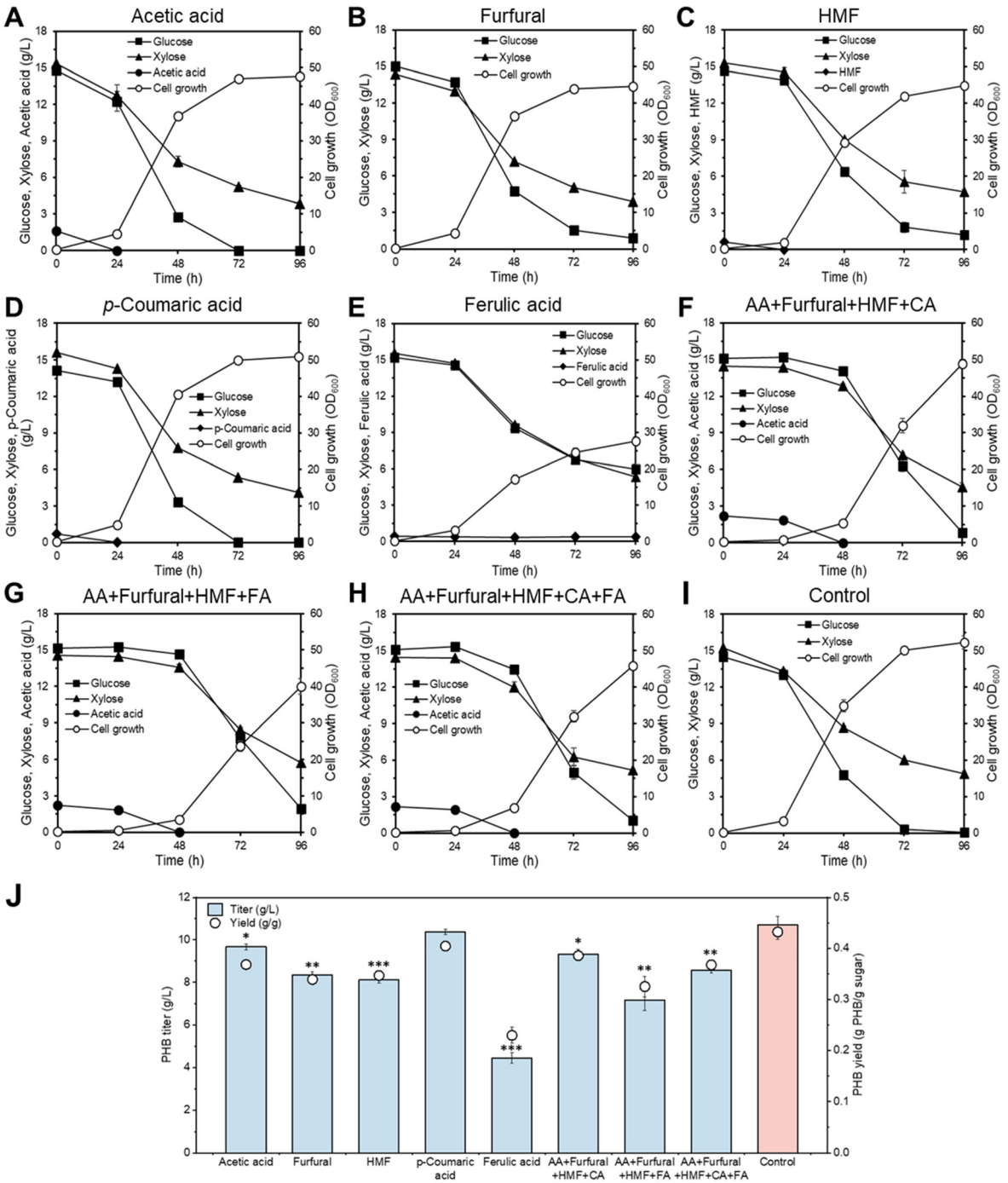

Fig. 4 Effects of individual and combined lignocellulosic hydrolysate-derived inhibitors on the fermentation performance of *C. necator* RXI22 under mixed-sugar conditions. Cell growth and sugar utilization profiles of RXI22 cultivated in minimal medium containing 15 g L^{-1} glucose and 15 g L^{-1} xylose with (A) 1.5 g L^{-1} acetic acid, (B) 0.02 g L^{-1} furfural, (C) 0.5 g L^{-1} HMF, (D) 0.5 g L^{-1} *p*-coumaric acid, (E) 0.5 g L^{-1} ferulic acid, (F) AA + furfural + HMF + CA, (G) AA + furfural + HMF + FA, (H) AA + furfural + HMF + CA + FA, and (I) a control without inhibitors. (J) PHB titer and yield after 96 h of cultivation. For combined-inhibitor conditions, each inhibitor was supplied at the same concentration used in the corresponding single-inhibitor experiments. When both phenolic compounds were added simultaneously, each was supplied at 0.25 g L^{-1} (total phenolics 0.5 g L^{-1}). Data are presented as mean ± standard deviation of three biological replicates. Abbreviations: AA, acetic acid; HMF, 5-hydroxymethylfurfural; FA, ferulic acid; CA, *p*-coumaric acid. Statistical significance was determined using Student's two-tailed *t*-test by comparing each inhibitor-supplemented group against the inhibitor-free control (*, $p < 0.05$; **, $p < 0.01$; ***, $p < 0.001$).

imposed more noticeable effects than acetic acid, lowering PHB yields to 0.34 g g^{-1} and titers to 8.1–8.4 g L^{-1} (Fig. 4B, C and J). While HMF (initial concentration of 0.5 g L^{-1}) was explicitly presented in the fermentation profiles, furfural data were omitted due to its low initial concentration (0.02 g L^{-1}). Nevertheless, complete depletion of both furanic compounds was confirmed within 24 h. These inhibitory effects are typically attributed to the interference of furans with key metabolic enzymes. However, their impact was transient as *C. necator* possesses the metabolic capacity to detoxify these inhibitors to less toxic alcohols.[44,45]

In contrast, the two phenolic compounds showed markedly distinct behaviors. *p*-Coumaric acid was rapidly consumed and supported cell growth and PHB production comparable to the control (Fig. 4D), consistent with previous findings that *C. necator* can metabolize this compound at low levels.[46] Conversely, ferulic acid caused pronounced inhibition, leaving 6.0 g L^{-1} glucose unconsumed after 96 h and reducing PHB titers (4.5 g L^{-1}) and yields (0.23 g g^{-1}) to less than half of the control (Fig. 4E and J). Unlike *p*-coumaric acid, 0.5 g L^{-1} of the ferulic acid remained unutilized in the medium throughout the cultivation period (Fig. 4E). This disparity in inhibitory strength between the two phenolics likely stems from their structural differences. Ferulic acid possesses a methoxy group that requires an *O*-demethylation step for its metabolism, rendering it more recalcitrant to degradation by the strain compared to *p*-coumaric acid.[47] Consequently, the prolonged presence of ferulic acid induces severe cellular stress including membrane disruption and oxidative damage, thereby significantly impairing both primary metabolism and PHB biosynthesis.[45,48]

When inhibitors were added in combination to simulate hydrolysate conditions, synergistic inhibition emerged. Mixed inhibitors caused substantial delays in utilization of both glucose and xylose and resulted in pronounced reductions in cell growth, indicating combined metabolic and stress-response burdens (Fig. 4F–H). Acetic acid consumption was also delayed under mixture conditions; however, PHB titers were not further reduced beyond levels observed for individual inhibitors, indicating that its contribution to PHB inhibition is minor relative to other compounds. Interestingly, ferulic acid alone produced the strongest overall inhibition, whereas its effect was partially alleviated when combined with other inhibitors, suggesting antagonistic or stress-induced compensatory interactions, consistent with earlier observations.[49–51] Overall, these findings suggest that the inhibitory impact of phenolics is closely linked to their metabolic accessibility. While *p*-coumaric acid is rapidly attenuated, others as exemplified by ferulic acid persist longer in the medium. This prolonged presence results in sustained cellular stress, making such persistent phenolic derivatives major contributors to the reduced performance in actual hydrolysates. Importantly, the inhibition patterns observed under hydrolysate-like conditions were not simply additive but arose from the combined effects of mixed-sugar metabolism and interactions among multiple inhibitors.

3.5. Enhanced performance of *C. necator* RXI22 under hydrolysate-derived inhibitory stress by addition of nicotinic acid and tryptophan

As discussed above, lignocellulosic hydrolysates contain multiple inhibitory compounds that impair microbial growth and metabolism, ultimately limiting overall bioprocess efficiency. To mitigate these inhibitory effects, various strategies have been explored including process-based approaches such as short-term adaptive cultivation and pretreatment optimization, as well as supplementation with tolerance-enhancing divalent metal ions (*e.g.*, Mg^{2+} and Ca^{2+}).[52–54] In parallel, synthetic biology and metabolic engineering approaches have also been applied to strengthen microbial robustness under inhibitor-rich conditions.[35] Those studies suggested that modulation of intracellular cofactors such as NAD^+-related biosynthetic pathways can enhance microbial tolerance to environmental and metabolic stress.[12,55] Based on these findings, we hypothesized that a simple nutritional supplementation strategy would prevent the inhibitor-induced performance losses in *C. necator* RXI22. To test the hypothesis, we evaluated external supplementation with two metabolites involved in cellular cofactor metabolism, nicotinic acid and tryptophan,[56,57] as readily implementable additives to support cellular function under the inhibitory conditions.

To rapidly assess their individual effects, nicotinic acid and tryptophan were first tested in small-scale culture tubes. Each compound was supplemented at concentrations of 0.5, 1, and 2 g L^{-1} in 3 mL of minimal medium containing a defined mixture of inhibitors. Glucose and xylose were provided at 7.5 g L^{-1} each, and inhibitory compounds were added at concentrations that most closely reproduced the fermentation performance observed in hydrolysate-based cultures, specifically acetic acid (1.5 g L^{-1}), furfural (0.02 g L^{-1}), HMF (0.5 g L^{-1}), and ferulic acid (0.5 g L^{-1}). Interestingly, tryptophan consistently promoted higher cell growth compared to nicotinic acid, resulting in up to a 34% increase in OD_{600} relative to the control after 72 h (Fig. S3). These observations suggested that supplementation with nicotinic acid or tryptophan could partially improve RXI22 growth under inhibitory conditions, providing the rationale for subsequent flask-scale experiments with an expanded concentration range to further assess their effects on inhibitor tolerance.

When the tryptophan supplementation range was expanded from 0.05 to 2 g L^{-1}, the most pronounced improvements in both cell growth and PHB production were observed at 0.1 and 0.3 g L^{-1} (Fig. 5). At these concentrations, *C. necator* RXI22 reached biomass levels of 11.1–11.3 g L^{-1} and produced 8.3–8.4 g L^{-1} of PHB, corresponding to yields of 0.34–0.36 g g^{-1}. Compared with the control culture (7.2 g L^{-1} PHB from 10.0 g L^{-1} biomass), these conditions resulted in 11–13% higher cell mass and a 15–17% increase in PHB titer. The enhanced performance at optimal tryptophan levels may be associated with enhanced cellular robustness under inhibitory conditions. Given that tryptophan participates in NAD^+ biosynthetic pathways, supplementation could contribute to main-

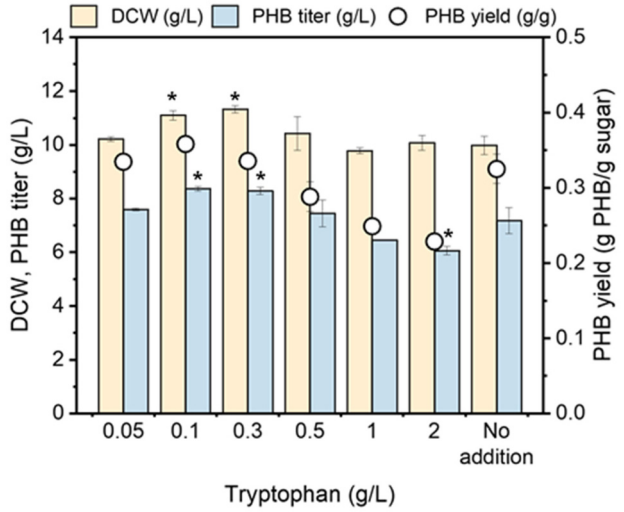

Fig. 5 Effect of tryptophan supplementation on the growth and PHB production of *C. necator* RXI22 under inhibitor-stressed mixed-sugar conditions. Dry cell weight (DCW), PHB titer, and yield were determined after 96 h of cultivation. Cultures were grown on a mixed-sugar substrate consisting of glucose (15 g L^{-1}) and xylose (15 g L^{-1}) with tryptophan supplementation ranging from 0.05 to 2 g L^{-1}. The inhibitor mixture, acetic acid (1.5 g L^{-1}), furfural (0.02 g L^{-1}), HMF (0.5 g L^{-1}), and ferulic acid (0.5 g L^{-1}), was formulated to mimic the inhibitory environment of lignocellulosic hydrolysate fermentations. Data are presented as mean ± standard deviation of three biological replicates. Student's two-tailed *t*-test was performed to determine the significance of differences between the tryptophan-supplemented groups and the non-supplemented control (*, $p < 0.05$).

taining a more favorable intracellular redox balance under stress. In addition, because tryptophan biosynthesis is energetically demanding, external supplementation of tryptophan may reduce metabolic burden, thereby allowing increased allocation of cellular resources toward growth and PHB accumulation.[58] At higher tryptophan concentrations, however, both cell growth and PHB production declined. This trend may be associated with changes in the effective C/N ratio, as amino acids can serve as a nitrogen source at a high concentration.[59] Such shifts could disrupt metabolic balance and ultimately constrain production.[60] Overall, these results indicate that tryptophan supplementation improves tolerance and productivity only within a defined concentration window.

The tryptophan supplementation strategy was next evaluated in fermentations using lignocellulosic hydrolysates to assess its effectiveness under more realistic process conditions. However, when sugarcane bagasse and rice straw hydrolysates were supplemented with 0.1 and 0.3 g L^{-1} tryptophan, no significant improvements in either cell growth or PHB production were observed (Fig. S4). This outcome can be attributed to the presence a broader and more complex array of inhibitory compounds in actual hydrolysates, whose combined effects cannot be sufficiently alleviated by tryptophan supplementation alone. Similar discrepancies have been noted in previous studies, where metal-ion supplementation enhanced fermentation performance in defined media but showed limited effectiveness in hydrolysate-based fermentations, underscoring the challenge posed by multifactorial inhibitory stress.[54]

In this study, we employed a simple nutritional supplementation strategy to improve fermentation performance. While such approaches offer practical benefits, including ease of implementation and compatibility with existing bioprocesses, their indirect mode of action limits their ability to counter the diverse inhibitory stresses present in lignocellulosic hydrolysates. Thus, achieving more robust and consistent improvements will likely require combining process-level optimization with metabolic engineering strategies that strengthen intracellular detoxification capacity and broaden the strain's capacity to metabolically mitigate inhibitory compounds. Beyond metabolic robustness, the phenotypic stability of an engineered strain is a critical factor for industrial viability. In this study, the *C. necator* RXI22 strain exhibited consistent phenotypic performance across repeated cultivations under identical conditions, with coefficients of variation for biomass and PHB production remaining below 5%. This stability is likely attributed to the chromosomal integration of the xylose assimilation pathway, which reduces the risk of trait loss compared to plasmid-based systems. To ensure readiness for large-scale industrial applications, future studies should incorporate systematic long-term stability tests, including extensive serial passaging and genome re-sequencing, to thoroughly verify genetic integrity.

4. Conclusions

This study demonstrates that the engineered *C. necator* strain RXI22 serves as a robust microbial platform for PHB production from lignocellulosic sugars. *C. necator* RXI22 exhibited stable cell growth and PHB biosynthesis across varying glucose–xylose ratios. When cultivated on sugarcane bagasse and rice straw hydrolysates, RXI22 achieved PHB yields of 0.29–0.30 g g^{-1}, confirming its compatibility with real biomass-derived feedstocks, although overall performance declined compared with the synthetic mixed sugars (0.42–0.43 g g^{-1}). Comprehensive inhibitor profiling further revealed that phenolic compounds imposed the most severe inhibition, followed by furan derivatives and acetic acid. A simple nutritional supplementation approach partially alleviated stress imposed by model inhibitor mixtures, improving both growth and PHB production. However, these benefits did not extend to actual hydrolysate fermentations, suggesting that medium-level adjustments alone may be insufficient to overcome the complex inhibitor matrix present in real biomass hydrolysates. Overall, this work demonstrates a promising microbial platform for lignocellulose-based PHB biomanufacturing. Future research should focus on further elucidating the underlying inhibitory mechanisms of complex lignocellulosic hydrolysates and developing more robust strains through targeted metabolic engineering. For example, enhancing specific phenolic detoxification pathways could significantly improve

lignocellulosic fermentation performances. The identified bioprocess-level bottlenecks provide key insights to guide future strain development as well as pretreatment process development.

Author contributions

Habin Sun: writing – original draft, visualization, methodology, investigation, formal analysis, data curation, conceptualization. So Jeong Lee: visualization, methodology, investigation, formal analysis, data curation, conceptualization. Hyun-Joong Kim: methodology. Hyeongmin Seo, Jeongchan Lee, Jung Ho Ahn, Gyeongtaek Gong, Youngsoon Um, Kyoung Heon Kim: writing – review & editing. Ja Kyong Ko: writing – review & editing, supervision, project administration, funding acquisition, conceptualization.

Conflicts of interest

There are no conflicts to declare.

Data availability

All data supporting this study are included in the article and its supplementary information (SI). Supplementary information is available. See DOI: https://doi.org/10.1039/d6gc01068g.

Acknowledgements

This research was supported by the Bio & Medical Technology Development Program of the National Research Foundation (NRF), funded by the Korean government (MSIT) (no. RS-2024-00451875), and the Global Center for Sustainable Bioproducts with the National Science Foundation Office of International Science and Engineering (NSF OISE 2435227). The authors also appreciate the additional support provided by the Korea Institute of Science and Technology (KIST) Institutional Programs (26E0311).

References

1 K. Olonisakin, A. K. Mohanty, M. Thimmanagari and M. Misra, *Green Chem.*, 2025, **27**, 11656–11704.
2 S. S. Ali, T. Elsamahy, E. A. Abdelkarim, R. Al-Tohamy, M. Kornaros, H. A. Ruiz, T. Zhao, F. H. Li and J. Z. Sun, *Bioresour. Technol.*, 2022, **363**, 127869.
3 A. Mokhtarzadeh, A. Alibakhshi, M. Hejazi, Y. Omidi and J. E. N. Dolatabadi, *TrAC, Trends Anal. Chem.*, 2016, **82**, 367–384.
4 S. Behera, M. Priyadarshanee, Vandana and S. Das, *Chemosphere*, 2022, **294**, 133723.
5 E. Vlaeminck, E. Uitterhaegen, K. Quataert, T. Delmulle, K. De Winter and W. K. Soetaert, *World J. Microbiol. Biotechnol.*, 2022, **38**, 238.
6 F. H. Isikgor and C. R. Becer, *Polym. Chem.*, 2015, **6**, 4497–4559.
7 H. J. Lee, H. J. Jung, B. Kim, D. H. Cho, S. H. Kim, S. K. Bhatia, R. Gurav, Y. G. Kim, S. W. Jung, H. J. Park and Y. H. Yang, *Int. J. Biol. Macromol.*, 2023, **225**, 757–766.
8 R. C. R. Suplito, P. J. Requiso, C. G. Alfafara, F. R. P. Nayve Jr and J.-R. Ventura, *Biocatal. Agric. Biotechnol.*, 2025, 103634.
9 C. H. Zhou, X. Xia, C. X. Lin, D. S. Tong and J. Beltramini, *Chem. Soc. Rev.*, 2011, **40**, 5588–5617.
10 S. L. Riedel, J. N. Lu, U. Stahl and C. J. Brigham, *Appl. Microbiol. Biotechnol.*, 2014, **98**, 1469–1483.
11 N. Annamalai and N. Sivakumar, *J. Biotechnol.*, 2016, **237**, 13–17.
12 S. M. Lee, D. H. Cho, H. J. Jung, B. Kim, S. H. Kim, S. K. Bhatia, R. Gurav, J. M. Jeon, J. J. Yoon, J. H. Park, J. H. Park, Y. G. Kim and Y. H. Yang, *Bioprocess Biosyst. Eng.*, 2022, **45**, 1719–1729.
13 I. Orita, R. Iwazawa, S. Nakamura and T. Fukui, *J. Biosci. Bioeng.*, 2012, **113**, 63–69.
14 S. J. Lee, J. Kim, J. H. Ahn, G. Gong, Y. Um, S.-M. Lee, K. H. Kim and J. K. Ko, *Bioresour. Technol.*, 2025, **418**, 131996.
15 J. H. Kim, D. E. Block and D. A. Mills, *Appl. Microbiol. Biotechnol.*, 2010, **88**, 1077–1085.
16 S. K. Bhatia, R. Gurav, T. R. Choi, H. R. Jung, S. Y. Yang, Y. M. Moon, H. S. Song, J. M. Jeon, K. Y. Choi and Y. H. Yang, *Bioresour. Technol.*, 2019, **271**, 306–315.
17 R. Chen, Y. Z. Wang, Q. Liao, X. Zhu and T. F. Xu, *BMB Rep.*, 2013, **46**, 244–251.
18 H. J. Kim, Y. B. Han, G. Lim, H. G. Koh, S. H. Park, K. Park, S. K. Bhatia and Y. H. Yang, *Biochem. Eng. J.*, 2025, **222**, 109840.
19 J. K. Ko, T. Enkh-Amgalan, G. Gong, Y. Um and S. M. Lee, *GCB Bioenergy*, 2019, **12**, 90–100.
20 F. L. Wang and S. Y. Lee, *Appl. Environ. Microbiol.*, 1997, **63**, 3703–3706.
21 V. Kachrimanidou, N. Kopsahelis, S. Papanikolaou, I. K. Kookos, M. De Bruyn, J. H. Clark and A. A. Koutinas, *Bioresour. Technol.*, 2014, **172**, 121–130.
22 W. Hauf, M. Schlebusch, J. Huege, J. Kopka, M. Hagemann and K. Forchhammer, *Metabolites*, 2013, **3**, 101–118.
23 L. Zhang, Z. C. Jiang, T. H. Tsui, K. C. Loh, Y. J. Dai and Y. W. Tong, *Front. Bioeng. Biotechnol.*, 2022, **10**, 946085.
24 Y. H. Yang, C. J. Brigham, C. F. Budde, P. Boccazzi, L. B. Willis, M. A. Hassan, Z. A. M. Yusof, C. Rha and A. J. Sinskey, *Appl. Microbiol. Biotechnol.*, 2010, **87**, 2037–2045.
25 H. Al-Battashi, N. Annamalai, S. Al-Kindi, A. S. Nair, S. Al-Bahry, J. P. Verma and N. Sivakumar, *J. Clean. Prod.*, 2019, **214**, 236–247.
26 H. S. Kim, Y. H. Oh, Y. A. Jang, K. H. Kang, Y. David, J. H. Yu, B. K. Song, J. I. Choi, Y. K. Chang, J. C. Joo and S. J. Park, *Microb. Cell Fact.*, 2016, **15**, 95.

27 T. Xu, H. Li, S. J. Zhang, Q. Xue, R. Hewage, J. H. Wang, F. Guo, D. H. Zhao, G. M. Ai, D. Kahramon, H. Xiang and J. Han, *Bioresour. Technol.*, 2025, **424**, 132276.
28 X. Kourilova, I. Pernicova, K. Sedlar, J. Musilova, P. Sedlacek, M. Kalina, M. Koller and S. Obruca, *Bioresour. Technol.*, 2020, **315**, 123885.
29 A. Matsushika, A. Nagashima, T. Goshima and T. Hoshino, *PLoS One*, 2013, **8**, e69005.
30 Y. H. Zhang, W. D. Sun, H. W. Wang and A. L. Geng, *Bioresour. Technol.*, 2013, **147**, 307–314.
31 R. D. Ashby, D. K. Y. Solaiman, A. Nuñez, G. D. Strahan and D. B. Johnston, *Bioresour. Technol.*, 2018, **253**, 333–342.
32 S. I. Mussatto and I. C. Roberto, *Bioresour. Technol.*, 2004, **93**, 1–10.
33 R. Kanzariya, A. Gautam, S. Parikh, M. L. Shah and S. Gautam, *Biotechnol. Genet. Eng. Rev.*, 2024, **40**, 1113–1135.
34 N. Annamalai, H. Al-Battashi, S. Al-Bahry and N. Sivakumar, *J. Biotechnol.*, 2018, **265**, 25–30.
35 C. H. Weng, R. H. Tang, X. W. Peng and Y. J. Han, *Bioresour. Technol.*, 2023, **374**, 128762.
36 M. M. Khattab and Y. Dahman, *Bioprocess Biosyst. Eng.*, 2019, **42**, 1115–1127.
37 P. Millard, B. Enjalbert, S. Uttenweiler-Joseph, J. C. Portais and F. Létisse, *eLife*, 2021, **10**, e63661.
38 J. E. Gonzalez, C. P. Long and M. R. Antoniewicz, *Metab. Eng.*, 2017, **39**, 9–18.
39 P. Millard, T. Gosselin-Monplaisir, S. Uttenweiler-Joseph and B. Enjalbert, *EMBO J.*, 2023, **42**, e113079.
40 F. Xu, R. C. Sun, J. X. Sun, C. F. Liu, B. H. He and J. S. Fan, *Anal. Chim. Acta*, 2005, **552**, 207–217.
41 X. X. Chen, Y. Y. Xue, J. J. Hu, Y. F. Tsang and M. T. Gao, *Appl. Biochem. Biotechnol.*, 2017, **183**, 685–698.
42 P. Cola, D. P. Procópio, A. T. D. Alves, L. R. Carnevalli, I. V. Sampaio, B. L. V. da Costa and T. O. Basso, *Biotechnol. Lett.*, 2020, **42**, 571–582.
43 X. Wang, E. B. Goh and H. R. Beller, *Microb. Cell Fact.*, 2018, **17**, 12.
44 Z. L. Liu, J. Moon, B. J. Andersh, P. J. Slininger and S. Weber, *Appl. Microbiol. Biotechnol.*, 2008, **81**, 743–753.
45 O. Ibraheem and B. K. Ndimba, *Int. J. Biol. Sci.*, 2013, **9**, 598–612.
46 W. Wang, S. H. Yang, G. B. Hunsinger, P. T. Pienkos and D. K. Johnson, *Front. Microbiol.*, 2014, **5**, 247.
47 Z. Chen, H. Liu, Q. J. Zong, T. X. Liang, J. Sun, T. Xu, Z. H. Liu, J. P. Wu, B. Z. Li and Y. J. Yuan, *ACS Sustainable Chem. Eng.*, 2024, **12**, 17726–17738.
48 S. Lee, J. H. Lee and R. J. Mitchell, *Biotechnol. Biofuels*, 2015, **8**, 68.
49 M. A. Franden, H. M. Pilath, A. Mohagheghi, P. T. Pienkos and M. Zhang, *Biotechnol. Biofuels*, 2013, **6**, 99.
50 L. van der Maas, J. L. S. P. Driessen and S. I. Mussatto, *Energies*, 2021, **14**, 8419.
51 D. Greetham, A. J. Hart and G. A. Tucker, *Biomass Bioenergy*, 2016, **85**, 53–60.
52 A. K. Chandel, S. S. da Silva and O. V. Singh, *BioEnergy Res.*, 2013, **6**, 388–401.
53 I. D. Bianchini, L. Sene, M. A. A. da Cunha and M. D. D. Felipe, *BioEnergy Res.*, 2022, **15**, 1182–1194.
54 J. K. Ko, Y. Um and S. M. Lee, *Bioresour. Technol.*, 2016, **222**, 422–430.
55 H. L. Liu, C. H. T. Wang, E. P. I. Chiang, C. C. Huang and W. H. Li, *Biotechnol. Biofuels*, 2021, **14**, 200.
56 O. Kurnasov, V. Goral, K. Colabroy, S. Gerdes, S. Anantha, A. Osterman and T. P. Begley, *Chem. Biol.*, 2003, **10**, 1195–1204.
57 S. Johnson and S. i. Imai, *F1000Res.*, 2018, **7**, 132.
58 T. Patil, P. Bannerjee, A. Agarwal, A. D. Tripathi, V. Paul, A. Hooda, M. K. Gatasheh and D. K. Mahato, *Sci. Rep.*, 2025, **15**, 38638.
59 B. M. Pruss, J. M. Nelms, C. Park and A. J. Wolfe, *J. Bacteriol.*, 1994, **176**, 2143–2150.
60 Y. W. Cui, Y. P. Shi and X. Y. Gong, *RSC Adv.*, 2017, **7**, 18953–18961.